The Winding Stray Field of Large Power Transformers – An Analytical Approach

Erich Schmidt, Peter Hamberger

Proceedings of the
26th International Conference on Applied Computational Electromagnetics (ACES),
CD-ROM, 2010

The Winding Stray Field of Large Power Transformers — An Analytical Approach

Erich Schmidt[1] and Peter Hamberger[2]

[1]Institute of Electrical Drives and Machines, Vienna University of Technology, Vienna, Austria
erich.schmidt@tuwien.ac.at

[2]Siemens Transformers Austria Ltd., Linz, Austria
peter.hamberger@siemens.com

Abstract: To meet the increasing requirements with the initial design of large power transformers, a novel analytical approach for determining the stray field of low and high voltage as well as tapping windings is presented. The algorithm solves for the 3D Laplacian equation of the 3D magnetic vector potential by using series expansions according to the orthogonal Eigenfunctions of the related Eigenvalue problem. The main interest lies on a very fast calculation method which can be used as a criteria for the selection of winding arrangement and tank wall geometry with the initial design.

Keywords: Eigenfunction expansion, Stray field calculation, Power transformers

1. Introduction

To maintain quality, performance and competiveness, an improvement of the calculation methods used with the initial design will meet the increasing requirements and challenges in the design of large power transformers. Short-term customer deadlines and individual customer demands require high levels of precision and reliability of those calculation results. The main focus of such enhanced design tools lies on a very fast calculation method which can be used as a criteria for the selection of winding arrangement and tank wall geometry in the initial design.

Former basic analytical calculations, eg. [1]–[3], use many simplifications which are not suitable for the purpose given above. On the other hand, fully numerical approaches, such as [4]–[6], cannot overcome the drawbacks of 3D numerical analysis methods when concerning the details of the winding structures of modern large power transformers. Due to their high efforts with modelling and simulation, they are not applicable for the initial design.

Therefore, a novel analytic method for determining the stray field of large power transformers is presented which takes into account for the detailed configuration of both low and high voltage windings as well as tapping windings. The algorithm solves for the 3D Laplacian equation of the 3D magnetic vector potential by using series expansions according to the orthogonal Eigenfunctions of the related Eigenvalue problem. The effects of the high permeable laminated iron core are represented by appropriate boundary conditions for the 3D magnetic vector potential at the boundaries of the iron core. In order to fulfil these boundary conditions, fictious surface currents at the iron core boundaries are introduced. In summary, the 3D magnetic vector potential will be obtained from one main part generated by the currents of the windings and another main part produced from the surface currents representing the iron core boundaries.

2. Governing Equations

Starting from the Maxwell equations and their interface conditions [7], [8]

$$\operatorname{curl}\mathbf{H} = \mathbf{J} \ , \quad \mathbf{n} \times [\![\mathbf{H}]\!] = \mathbf{K} \ , \tag{1}$$

$$\operatorname{div}\mathbf{B} = 0 \quad , \quad \mathbf{n} \cdot [\![\mathbf{B}]\!] = 0 \ , \tag{2}$$

a gauged magnetic vector potential will be introduced,

$$\mathbf{B} = \operatorname{curl}\mathbf{A} \ , \quad \operatorname{div}\mathbf{A} = 0 \ . \tag{3}$$

Based on the cartesian coordinate system of the arrangement $0<x<x_0$, $0<y<y_0$, $0<z<z_0$ as shown in Fig. 1, the vector Laplacian equation outside of the core regions reads as

$$-\nabla\!\!\!\nabla\mathbf{A}(x,y,z) = \mu_0\,\mathbf{J}(x,y,z) \tag{4}$$

and the components of the magnetic vector potential are separated using the scalar Laplacian operator,

$$-\Delta A^{(i)}(x,y,z) = \mu_0\,J^{(i)}(x,y,z)\ ,\quad i=x,y,z\ . \tag{5}$$

Consequently, these equations can be solved for each component of the magnetic vector potential independently.

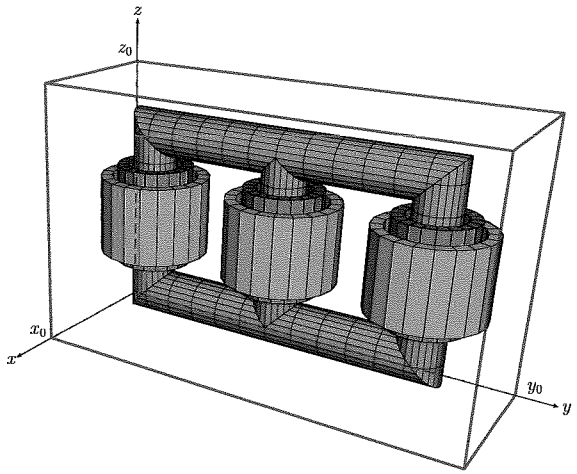

Fig. 1: Schematic of a three leg transformer inside the tank wall planes.

Table 1:
Boundary Conditions at the Tank Wall Planes.

non-conductive tank wall: $\mathbf{n}\times\mathbf{B}=\mathbf{0}$
$\frac{\partial}{\partial n}(\mathbf{n}\times\mathbf{A})=\mathbf{0}$
$\mathbf{n}\cdot\mathbf{A}=0$
conductive tank wall: $\mathbf{n}\cdot\mathbf{B}=0$
$\mathbf{n}\times\mathbf{A}=\mathbf{0}$
$\frac{\partial}{\partial n}(\mathbf{n}\cdot\mathbf{A})=0$

As listed in Table 1, two sets of boundary conditions are considered on the tank wall planes. First, the magnetic flux density has only a normal component at the tank wall planes representing non-conductive infinite high permeable tank wall planes. Secondly, conductive infinite high permeable tank wall planes generate surface current densities which yield only a tangential magnetic flux density at the tank wall planes.

Corresponding to these two limiting cases, the components of the magnetic vector potential will fulfil either homogeneous Dirichlet or Neumann boundary conditions on the tank wall planes. In particular, at least one Dirichlet boundary condition exists for each component of the magnetic vector potential.

3. Eigenvalue Problem

The Eigenvalue problem [9] for the cube $0<x<x_0$, $0<y<y_0$, $0<z<z_0$ formed by the tank wall planes is given by

$$-\Delta u(x,y,z) = \lambda\,u(x,y,z)\ . \tag{6}$$

According to the boundary conditions listed in Table 1, for $k,l,m=0,1,2,\ldots$ the general Eigenvalues

$$\lambda_{klm} = \left(\frac{k\pi}{x_0}\right)^2+\left(\frac{l\pi}{y_0}\right)^2+\left(\frac{m\pi}{z_0}\right)^2 > 0 \tag{7}$$

define the general normalized Eigenfunctions

$$u_{klm}(x,y,z) = u_k(x)\,u_l(y)\,u_m(z) \tag{8}$$

with

$$u_k(x) = \sqrt{\frac{2-\delta_{k0}}{x_0}}\,\mathrm{trig}\frac{k\pi x}{x_0}\ ,\quad u_l(y) = \sqrt{\frac{2-\delta_{l0}}{y_0}}\,\mathrm{trig}\frac{l\pi y}{y_0}\ ,\quad u_m(z) = \sqrt{\frac{2-\delta_{m0}}{z_0}}\,\mathrm{trig}\frac{m\pi z}{z_0}\ , \tag{9}$$

where trig = sin with Dirichlet boundary conditions and trig = cos with Neumann boundary conditions.

Hence, the general Eigenvalues (7) and the general Eigenfunctions (8) related to the boundary conditions listed in Table 1 yield the Green's functions

$$G^{(i)}(\mathbf{x},\boldsymbol{\xi}) = \sum_{k,l,m} \frac{u^{(i)}_{klm}(x,y,z)\, u^{(i)}_{klm}(\xi,\eta,\zeta)}{\lambda_{klm}} \tag{10}$$

separated for each component of the magnetic vector potential $A^{(i)}$. These Green's functions allow for the calculation of the components of the magnetic vector potential from

$$A^{(i)}(\mathbf{x}) = \int_{\Omega} G^{(i)}(\mathbf{x},\boldsymbol{\xi})\, \mu_0 J^{(i)}(\boldsymbol{\xi})\, d\Omega_{\xi,\eta,\zeta} + \oint_{\Gamma} G^{(i)}(\mathbf{x},\boldsymbol{\xi})\, \mu_0 K^{(i)}(\boldsymbol{\xi})\, d\Gamma_{\xi,\eta,\zeta} \ , \tag{11}$$

which fulfil the boundary conditions listed in Table 1.

4. Setup of the General Solution

As shown with (11) for each component, the total magnetic vector potential and subsequently the magnetic field strength can be constructed from two parts,

$$\mathbf{A}(\mathbf{x}) = \mathbf{A}_J(\mathbf{x}) + \mathbf{A}_K(\mathbf{x}) \ , \tag{12}$$

$$\mathbf{H}(\mathbf{x}) = \mathbf{H}_J(\mathbf{x}) + \mathbf{H}_K(\mathbf{x}) \ . \tag{13}$$

The first parts $\mathbf{A}_J(\mathbf{x})$,$\mathbf{H}_J(\mathbf{x})$ encounter for any source current flow related to the various windings on the three legs of the power transformer. The second parts $\mathbf{A}_K(\mathbf{x})$,$\mathbf{H}_K(\mathbf{x})$ take into account any surface current densities on the boundaries. This fact can be used to encounter for the effects caused by the high permeable laminated iron core where the tangential components of magnetic flux density and magnetic field strength vanishes.

A. Source Field Terms

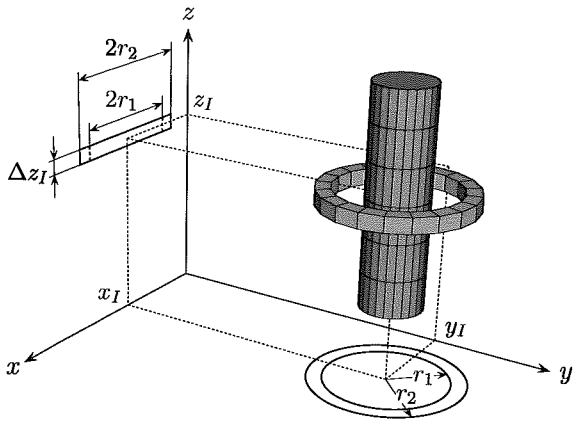

Fig. 2: Arrangement of one arbitrary winding on one of the three legs.

Let us first consider the calculation for one arbitrary winding on one of the three legs as depicted in Fig. 2. The single winding carries the total current I_I uniformly in circumferential direction. The respective source current region Ω_I is described by the local coordinates

$$r_1 < r < r_2 \ , \quad -\pi < \varphi < \pi \ , \qquad -\frac{\Delta z_I}{2} < z - z_I < \frac{\Delta z_I}{2} \tag{14}$$

and the local coordinate transformation

$$x(r,\varphi) = x_I + r\cos\varphi \ , \tag{15a}$$

$$y(r,\varphi) = y_I + r\sin\varphi \ . \tag{15b}$$

The corresponding part of the magnetic vector potential reads as

$$A^{(i)}_J(\mathbf{x};I_I) = I_I \sum_{k,l,m} \frac{a^{(i)}_{klm}}{\lambda_{klm}}\, u^{(i)}_{klm}(x,y,z) \ , \quad a^{(i)}_{klm} = \frac{\mu_0}{I_I} \int_{\Omega_I} J^{(i)}(\xi,\eta,\zeta)\, u^{(i)}_{klm}(\xi,\eta,\zeta)\, d\Omega_{\xi,\eta,\zeta} \ . \tag{16}$$

Using the Eigenfunctions (8) and the Bessel functions of integer order $J_n(z)$, the source field part of one winding carrying the total current I_I is represented by

$$a_{klm}^{(i)} = 2\pi\mu_0\, u_{klm}^{(i)}(x_I, y_I, z_I)\ \mathrm{si}\Big(\frac{m\pi\Delta z_I}{2\,z_0}\Big)\ \frac{\Big[r\sqrt{\lambda_{kl0}}\,J_0\big(r\sqrt{\lambda_{kl0}}\big) - 2\sum_{n=0}^{\infty} J_{2n+1}\big(r\sqrt{\lambda_{kl0}}\big)\Big]\Big|_{r=r_1}^{r=r_2}}{(r_2 - r_1)\lambda_{kl0}}\ . \quad (17)$$

Due to the current flow in circumferential direction only, the component $A_J^{(z)}$ of the magnetic vector potential vanishes for this winding type. On the other hand, in the case of helical windings with low voltage tapping windings the source field part $\mathbf{A}_J(\mathbf{x})$ of the magnetic vector potential consists of all three components.

In summary, the source field part $\mathbf{A}_J(\mathbf{x})$ of the magnetic vector potential is obtained corresponding to all winding currents I_{Ij}, the winding schemata and the geometry data on the three legs as given by

$$A_J^{(i)}(\mathbf{x}) = \sum_j A_J^{(i)}(\mathbf{x}; I_{Ij})\ . \quad (18)$$

B. Boundary Field Terms

In the second step, the boundary condition for magnetic flux density and magnetic field strength along the boundaries Γ_C of the laminated iron core as shown in Fig. 3 will be satisfied. Due to the very high permeability, the tangential component of the total magnetic field strength vanishes at the iron core boundaries,

$$\mathbf{n} \times \mathbf{H}(\mathbf{x})\,\Big|_{\Gamma_C} = \mathbf{n} \times \Big(\mathbf{H}_J(\mathbf{x}) + \mathbf{H}_K(\mathbf{x})\Big)\Big|_{\Gamma_C} = \mathbf{0} \quad (19)$$

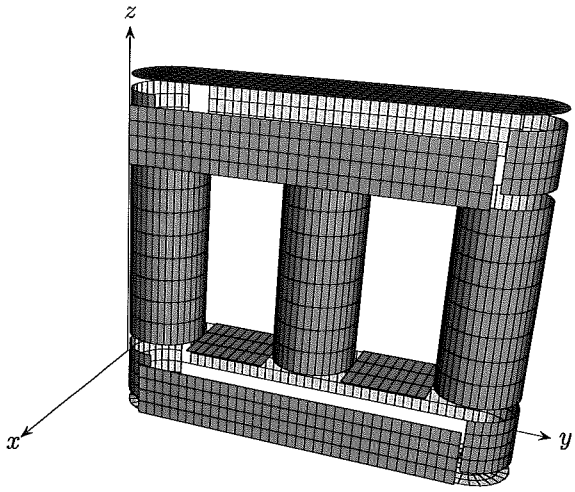

Fig. 3: Iron core boundary surfaces for the surface currents.

In general, the source field term generates a tangential component of the magnetic field strength at the iron core boundaries,

$$\mathbf{n} \times \mathbf{H}_J(\mathbf{x})\,\Big|_{\Gamma_C} \neq \mathbf{0}\ . \quad (20)$$

According to (1), this portion can be interpreted as a surface current density excitation

$$\mathbf{K}(\mathbf{x})\,\Big|_{\Gamma_C} = -\mathbf{n} \times \mathbf{H}_J(\mathbf{x})\,\Big|_{\Gamma_C} \quad (21)$$

for the second part of the vector potential $\mathbf{A}_K(\mathbf{x})$ in the sense that the total magnetic field strength as the sum of both parts has only a normal component on the iron core boundaries.

Consequently, the second part $\mathbf{A}_K(\mathbf{x})$ of the magnetic vector potential can be calculated from the surface integration of (11). Due to the fact that the iron core boundaries do not comply with the Eigenfunctions obtained from the Eigenvalue equation (6), the calculation of the second part $\mathbf{A}_K(\mathbf{x})$ cannot be done in a straightforward way. The surface current excitations at the iron core boundaries themselves generate portions of the magnetic field strength along the iron core boundaries. Therefore, the detailed distribution of the fictious surface currents $\mathbf{K}(\mathbf{x})$ is completely unknown and has to be determined according to the source field part caused by the winding currents.

In order to evaluate the unknown distribution of the fictious surface currents $\mathbf{K}(\mathbf{x})$, an edge based approximation of this distribution will be introduced at the iron core boundary surfaces. Each iron core boundary surface is discretized with a uniform mesh with constant mesh divisions Δx_M,Δy_M,Δz_M and

in case of the cylindrical surfaces on the legs additionally with $\Delta\varphi_M$ where $\pi/\Delta\varphi_M \in \mathcal{N}$. Along these surface discretizations, the surface current distribution will be approximated by uniform surface current components $K_E^{(i)}$ along the single edges and an appropriate interpolation between the edges.

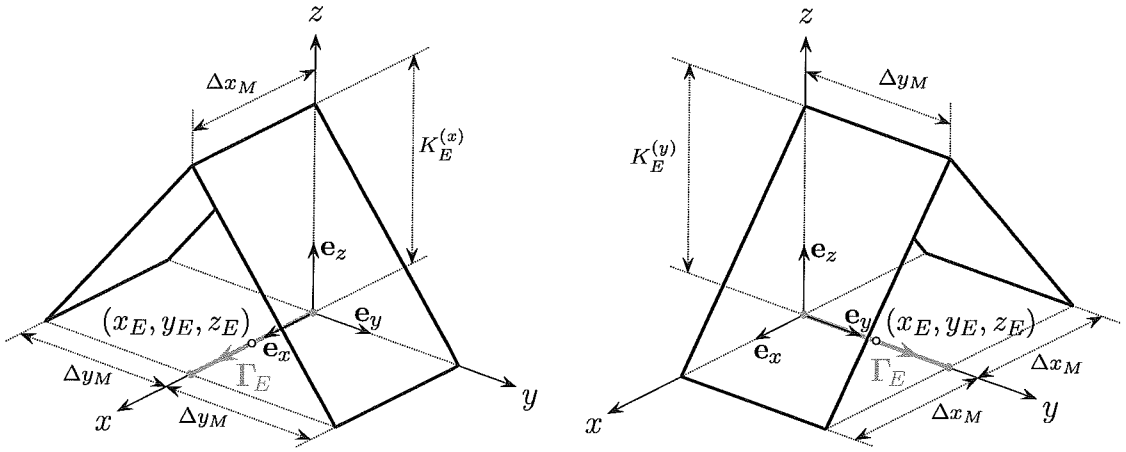

Fig. 4: Interpolation of the surface currents $K^{(x)}(x,y)$ (left part) and $K^{(y)}(x,y)$ (left part) along $z=z_E$.

As shown with Fig. 4 for a yoke surface with $\mathbf{n}=\mathbf{e}_z$, the edges Γ_E of the surface current region are described by the local coordinates

$$-\frac{\Delta x_M}{2} < x - x_E < \frac{\Delta x_M}{2} \;\;,\;\; y=y_E \;\;,\;\; z=z_E \tag{22}$$

for the x-direction and

$$x=x_E \;\;,\;\; -\frac{\Delta y_M}{2} < y - y_E < \frac{\Delta y_M}{2} \;\;,\;\; z=z_E \tag{23}$$

for the y-direction. The two interpolations along the appropriate edges

$$K^{(x)}(x,y) = K_E^{(x)}\Big(1 \pm \frac{y-y_E}{\Delta y_M}\Big) \;, \tag{24a}$$

$$K^{(y)}(x,y) = K_E^{(y)}\Big(1 \pm \frac{x-x_E}{\Delta x_M}\Big) \tag{24b}$$

guanrantee a divergence free distribution of the surface currents.

The corresponding part of the magnetic vector potential for each single edge Γ_E is obtained from

$$A_K^{(i)}(\mathbf{x}; K_E^{(i)}) = K_E^{(i)} \sum_{k,l,m} \frac{b_{klm}^{(i)}}{\lambda_{klm}}\, u_{klm}^{(i)}(x,y,z) \;\;,\;\; b_{klm}^{(i)} = \frac{\mu_0}{K_E^{(i)}} \int_{\Gamma_E} K^{(i)}(\xi,\eta,\zeta)\, u_{klm}^{(i)}(\xi,\eta,\zeta)\, d\Gamma_{\xi,\eta,\zeta} \;. \tag{25}$$

Using the Eigenfunctions (8), the surface field part of one single edge carrying the surface current $K_E^{(i)}$ at $z=z_E$ can be represented by

$$b_{klm}^{(x)} = \mu_0\, u_{klm}^{(x)}(x_E,y_E,z_E)\, \Delta x_M\, \Delta y_M\, \mathrm{si}\Big(\frac{k\pi\Delta x_M}{2\,x_0}\Big)\, \mathrm{si}^2\Big(\frac{l\pi\Delta y_M}{2\,y_0}\Big) \tag{26}$$

for the x-direction and

$$b_{klm}^{(y)} = \mu_0\, u_{klm}^{(y)}(x_E,y_E,z_E)\, \Delta x_M\, \Delta y_M\, \mathrm{si}^2\Big(\frac{k\pi\Delta x_M}{2\,x_0}\Big)\, \mathrm{si}\Big(\frac{l\pi\Delta y_M}{2\,y_0}\Big) \tag{27}$$

for the y-direction. The portions of the surface currents at the other iron core boundaries of the yokes and the three legs as shown in Fig. 3 are obtained from similar calculations.

In summary, the surface field part $\mathbf{A}_K(\mathbf{x})$ of the magnetic vector potential is obtained corresponding to all surface currents $K_{Ej}^{(i)}$ and their geometry data along all edges at the iron core boundaries as given by

$$A_K^{(i)}(\mathbf{x}) = \sum_{j_i} A_K^{(i)}(\mathbf{x}; K_{Ej}^{(i)}) \;. \tag{28}$$

C. Source and Boundary Field Terms

Due to the linearity of our problem in terms of both source and surface currents, the surface current distribution is strongly related to the total source current field of all windings. In summary, the complete vector potential $\mathbf{A}(\mathbf{x})$ and the complete magnetic field strength $\mathbf{H}(\mathbf{x})$ of all windings read as

$$A^{(i)}(\mathbf{x}) = \sum_j A_J^{(i)}(\mathbf{x}; I_{Ij}) + \sum_{j_i} A_K^{(i)}(\mathbf{x}; K_{Ej}^{(i)}) \ , \tag{29}$$

$$H^{(i)}(\mathbf{x}) = \sum_j H_J^{(i)}(\mathbf{x}; I_{Ij}) + \sum_{j_i} H_K^{(i)}(\mathbf{x}; K_{Ej}^{(i)}) \ . \tag{30}$$

Finally, (19) has to be fulfilled along all edges Γ_{Ej} at the iron core surface boundaries yielding an algebraic system of linear equations for the unknown fictious surface current components $K_{Ej}^{(i)}$ at the edges at the iron core surface boundaries. Since the describing matrix is singular, this algebraic system will be solved by an iterative method where the gauging condition for the magnetic vector potential will guarantee a unique solution for the distribution of the unknown surface currents.

5. Conclusion

The paper will discuss the evaluation of the stray field caused by each winding of large power transformers by using an analytical calculation method. The 3D magnetic vector potential is constructed from series expansions with regard to the Eigenvalue solutions of the 3D Laplacian equation within the region formed by the tank wall planes.

Thereby, the 3D magnetic vector potential consists of two portions. The first part represents the portion regarding the source current regions of the windings on the three legs. The second part encounters for the effects of the high permeable laminated iron core by assuming fictious surface currents to represent the appropriate boundary condition of the magnetic field on the iron core boundaries. Since this second part does not comply with the boundary conditions of the Eigenfunctions, an iterative method has to be used to finally obtain this second part of the complete 3D magnetic vector potential.

References

[1] M. Djurovic, C. Carpenter: "3-Dimensional Computation of Transformer Leakage Fields and Associated Losses". *IEEE Transactions on Magnetics*, Vol. 11, No. 5, September 1975.

[2] K. Zakrzewski, M. Lukaniszyn: "3-Dimensional Model of One- and Three-Phase Transformer for Leakage Field Calculation". *IEEE Transactions on Magnetics*, Vol. 28, No. 2, March 1992.

[3] K. Zakrzewski, B. Tomczuk: "Magnetic Field Analysis and Leakage Inductance Calculation in Current Transformers by Means of 3-D Integral Methods". *IEEE Transactions on Magnetics*, Vol. 32, No. 3, May 1996.

[4] N. Guangzheng, X. Xiaoming, C. Weiying, L. Gangru, J. Baidun, F. Zhenghu, L. Xianghua, X. Jitai: "FEM Analysis of 3-D Transformer Leakage Field and Eddy Current Loss in the Windings". *IEEE Transactions on Magnetics*, Vol. 28, No. 2, March 1992.

[5] L. Nowak, A. Demenko, W. Szelag: "Comparison of 3D and 2D Field-Circuit Models of Power Transformer Transients". *International Journal for Computation and Mathematics in Electrical and Electronic Engineering, COMPEL*, Vol. 23, No. 4, 2004.

[6] M. Breschi, A. Cristofolini: "Experimental and Numerical Analysis of Stray Field from Transformers". *IEEE Transactions on Magnetics*, Vol. 43, No. 11, November 2007.

[7] J.A. Stratton: *Electromagnetic Theory*. McGraw-Hill, New York, USA, 1941.

[8] J.D. Jackson: *Classical Electrodynamics*. Wiley, New York, USA, 1999.

[9] E.C. Titchmarsh: *Eigenfunction Expansions, Vol. I&II*. Oxford University Press, Cambridge, UK, 1958.